

## Vortex Multiplication in Applied Flow : the Precursor to Superfluid Turbulence

A.P.Finne,<sup>1</sup> V.B.Eltsov,<sup>1,2</sup> G.Eska,<sup>3</sup> R.Hanninen,<sup>4</sup> J.Kopu,<sup>1</sup> M.Krusius,<sup>1</sup> E.V.Thuneberg,<sup>5</sup> and M.Tsubota<sup>4</sup><sup>1</sup>Low Temperature Laboratory, Helsinki University of Technology, P.O.Box 2200, FIN-02015 HUT, Finland<sup>2</sup>Kapitza Institute for Physical Problems, Kosygina 2, 119334 Moscow, Russia<sup>3</sup>Physikalisches Institut, Universität Bayreuth, D-95440 Bayreuth, Germany<sup>4</sup>Department of Physics, Osaka City University, Osaka 558-8585, Japan<sup>5</sup>Department of Physical Sciences, P.O.Box 3000, FIN-90014 University of Oulu, Finland

(Dated: February 8, 2020)

The dynamics of quantized vortices in rotating  $^3\text{He-B}$  is investigated in the low density (single-vortex) regime as a function of temperature. An abrupt transition is observed at  $0.5T_c$ . Above this temperature the number of vortex lines remains constant, as they evolve to their equilibrium positions. Below this temperature the number of vortices increases linearly in time until the vortex density has grown sufficiently for turbulence to switch on. On the basis of numerical calculations we suggest a mechanism responsible for vortex formation at low temperatures and identify the mutual friction parameter which governs its abrupt temperature dependence.

PACS numbers: 67.40.Vs, 47.37.+q, 98.80.Cq

Measurements on bulk flow in superfluid  $^4\text{He-II}$  display typically irregular vortex formation at velocities much below the Landau limit of superfluidity. It is generally assumed that remanent vortices are initiated in externally applied flow and self-reconnect, producing new vortices. This process is seen in model calculations [1, 2], but direct comparison to pipe flow or rotating flow has proven controversial, unless strong surface pinning is invoked [1].

In  $^4\text{He-II}$  vortex motion is only weakly damped except at temperatures very close to  $T_c$ . New information on vortex formation is gained in  $^3\text{He-B}$  where both over- and underdamped regimes can be studied. Measurements on rotating flow show that in the strong damping regime at temperatures  $T > 0.6T_c$  vortex formation takes place at a well-defined critical velocity [3]. New vortices are formed in a flow instability and their number is conserved while they evolve towards their equilibrium configuration. In the weak damping conditions at  $T < 0.6T_c$  a sharp transition was found recently to a regime where the vortex number is not conserved: After the injection of a localized burst of 10 vortices into vortex-free flow, the vortex number was observed to increase abruptly [4]. This was interpreted as multiplication of the seed vortices through turbulence [5]. We call multiplication a process in which new vortices are formed as a result of the dynamic evolution of existing vortices.

Here we report on a new manifestation of the transition to multiplicative vortex dynamics below  $0.6T_c$ . In the regime of low vortex density and low applied flow velocity (compared to Ref. [4]) a prolonged increase in the number of vortices at constant rate is observed. This process appears as a precursor to turbulent vortex formation, building up the vortex density for turbulence to become possible in the bulk volume. A similar process is found in our numerical calculations of vortex motion. On the basis of the simulations, we attribute vortex formation in the low-density limit to the growth of unstable

Kelvin waves on isolated vortices and their reconnection with the sample boundary. This is different from the turbulent regime at higher vortex density where inter-vortex interactions in the bulk become important.

**Experiment:** Our sample of  $^3\text{He-B}$  is contained in a quartz tube of length  $d = 110\text{mm}$  and inner radius  $R = 3\text{mm}$ . The sample is rotated around its axis with angular velocity  $\Omega$ . In the lowest energy state a given number  $N$  of vortex lines are packed in a central cluster with areal density  $n = 2\pi/\Phi_0$ . Here  $\Phi_0 = h/2m_3$  is the circulation quantum. Outside the cluster there is counterflow of the normal and superfluid velocities,  $v_{cf} = v_n - v_s$ , which at the outer sample boundary has the largest magnitude  $v_{cfm} = [1/N(2\pi R^2)]R$ . Vortex lines form in an instability of the vortex-free flow only if  $v_{cfm}$  reaches the critical value  $v_c$ . In the present experiments  $v_c > 1\text{cm/s}$  at  $T < 0.8T_c$ . While  $v_{cfm} < v_c$  (which is always fulfilled in the measurements described here) growth of  $N$  can be attributed only to vortex multiplication.

The number of vortices in the cluster can be deduced independently at the top and bottom of the sample by measuring the NMR spectra using two spectrometers [6]. The technique is based on the strong dependence of the NMR spectrum on  $v_{cf}$ . By changing  $\Omega$  and  $T$  it is possible to compare the spectrum with specially prepared samples with known  $N$ . Alternatively, the texture of the B-phase order parameter and the spectrum can be calculated numerically [7] and comparison with experiments then gives  $N$ . The two methods are in good agreement.

The experimental signature of vortex multiplication is shown in Fig. 1. Here rotation is rapidly increased from a low angular velocity  $\Omega_i$  to a higher value  $\Omega_f$  and then kept constant. After reaching stable conditions,  $N$  first increases at a constant rate. At  $\Omega_f = 0.6\text{rad/s}$  this stage lasts for more than 200 s, generating approximately 1 vortex in 5 s until about 20% of the maximum number of vortices have been created. After this period vortices are

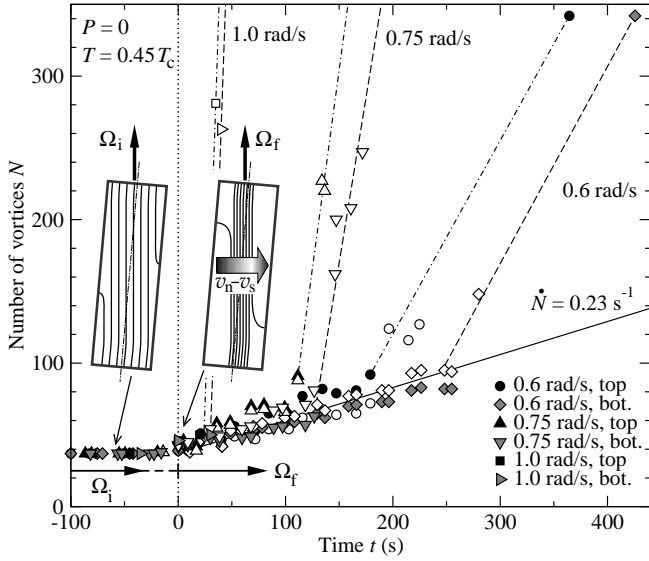


FIG. 1: Vortex formation in  $^3\text{He-B}$  at  $T < 0.5 T_c$ . The number of vortex lines  $N(t)$  in a cylindrical sample is shown. It is determined from NMR measurements at the top and the bottom of the sample using both experimental (filled data points) and theoretical (open data points) calibrations. Initially the sample is in equilibrium at an angular velocity  $\Omega_i = 0.05 \text{ rad/s}$  and contains  $N_i = 37$  vortices. Later  $\Omega$  is increased with a rate  $\dot{\Omega} = 0.025 \text{ rad/s}^2$  to a new stable value  $\Omega_f$ , which is reached at  $t = 0$ . During this ramp  $N$  is constant and the vortices are compressed to a central cluster around which the counterflow of the normal and superfluid components builds up (see schematic pictures in the inserts). Three runs with different  $\Omega_f$  are shown. The relaxation toward the equilibrium vortex state at  $\Omega_f$  ( $N_i = 430$  at  $0.6 \text{ rad/s}$  and  $750$  at  $1.0 \text{ rad/s}$ ) starts with a slow linear increase in  $N$  which later transforms to rapid turbulent multiplication of vortices. The solid line is the average vortex formation rate  $\dot{N}$  in the linear regime at  $\Omega_f = 0.6 \text{ rad/s}$ . The dashed lines are guides for the eye in the early part of turbulence. Vortex production in the pre-turbulent regime is attributed to instabilities of single vortices, which extend across the counterflow region and end at the cylindrical sample boundary (insert on the right). Such vortices exist in the initial state at  $\Omega_i$  due to misalignment of the sample and rotation axes (insert on the left).

formed at an accelerated rate until approximately the equilibrium number of vortices is reached. The latter stage is called turbulent because it is similar to observations in Ref. [4]. At larger  $\Omega_f$  the turbulent process sets in earlier: At  $\Omega_f = 1 \text{ rad/s}$  it starts already after 30 s from reaching constant rotation. The rate  $\dot{N}$  in the pre-turbulent regime increases as function of  $\Omega_i$ , but vortex formation is also observed when  $\Omega_i = 0$ .

The pre-turbulent vortex multiplication has the following experimentally established features: (i) The probability to observe vortex formation changes from zero to one in a narrow temperature interval as shown in Fig. 2. Here the transition temperature is about  $0.47 T_c$  for the case of  $\Omega_i = 0$ . The behavior when  $\Omega_i > 0$  is similar.

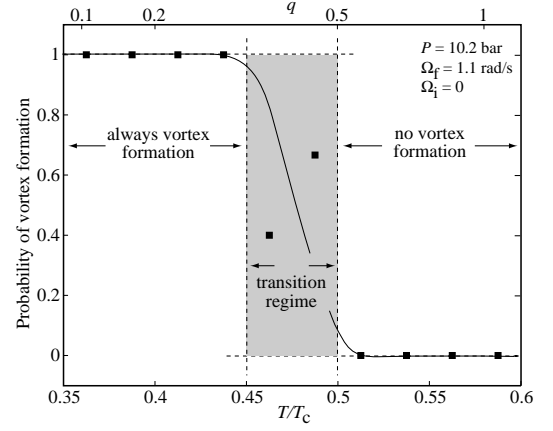


FIG. 2: The probability to observe vortex formation after rotation is increased from  $\Omega_i$  to  $\Omega_f$ , plotted vs. temperature (bottom axis) and mutual friction parameter  $q = (1 - \Omega_i^2 / \Omega_f^2)$  (top axis). No vortices are formed above  $0.5 T_c$ . Below  $0.45 T_c$  vortex formation of the type shown in Fig. 1 is always observed. At intermediate temperatures only part of the runs result in vortex formation. Here  $\Omega_i = 0$  is kept before each run for 4(12) minutes after deceleration from the state with vortex lines present. Dynamical arguments suggest that not all vortices are annihilated during this waiting time (see explanations in the text). The remnants generate new vortices when rotation is increased. The data consist of 32 measurements which are divided in bins of  $T = 0.025 T_c$  width. Angular velocity is increased to  $\Omega_f$  at constant rate  $\dot{\Omega} = (4 | 40) \cdot 10^3 \text{ rad/s}^2$ . Friction values are from Ref. [9].

(ii) Vortex formation proceeds independently in different parts of the sample: In the conditions of Fig. 1 it takes more than 300 s for a vortex created at one end of the sample to expand along the sample column and reach the other end [6]. Nevertheless vortex formation within the two NMR coils at the top and bottom of the sample is observed simultaneously.

(iii) The minimum flow velocity required for vortex multiplication is below the limit of our observations. The NMR technique loses sensitivity to  $N$  if the counterflow around the vortex cluster is small:  $v_{c, \text{min}} < 0.05 \text{ cm/s}$ .

(iv) Vortex multiplication at  $\Omega_f$  requires the presence of vortex lines connecting to the cylindrical sample boundary. Configurations without such vortices are prepared at  $T > 0.6 T_c$  as a vortex cluster with  $N$  less than the equilibrium number. While this cluster is separated by a wide counterflow region from the outer boundary the rotation velocity can be increased or decreased without vortex multiplication at any temperature down to  $0.35 T_c$ . When  $\Omega$  is decreased the vortex cluster expands towards the cylindrical sample boundary. If  $\Omega$  is decreased so that the cluster reaches the boundary (equilibrium vortex state) then on a subsequent increase of  $\Omega$ , while  $T < 0.5 T_c$ , vortex multiplication is observed.

Interpretation: Combining the experimentally established features with our analysis of vortex dynamics we

attribute the pre-turbulent vortex multiplication in Fig. 1 to an instability of a vortex line which connects to the cylindrical sample boundary. Such a vortex will be curved (as shown in the insert of Fig. 1) due to the competing influence of its image vorticity and rotation. We suggest that a curved vortex evolving in the applied flow may generate new vorticity in the following manner. The velocity  $v_L$  of a vortex line element is determined from [8]

$$v_L = v_s + \hat{s} \cdot (v_n - v_s) + \frac{1}{2} \hat{s} \cdot [\hat{s} \cdot (v_n - v_s)]: (1)$$

Here  $\hat{s}$  is a unit vector parallel to the vortex line element,  $v_n = \frac{1}{R} r$ , and  $\frac{1}{2}$  are mutual friction parameters measured in Ref. [9]. In our analysis we approximate a curved vortex segment with a circular loop of radius  $R_r$  and assume it to be initially perpendicular to the flow.

As can be seen from applying Eq. (1) such a vortex segment in rotational flow tends to develop line length along the flow at a rate  $(1 - \frac{1}{2})v_{si}$ , where  $v_{si} = \frac{1}{2}R_r$  is the self-induced velocity due to the vortex curvature. Here  $\frac{1}{2} = (\frac{1}{4}) \ln(R_r/a)$  ( $a$  is the vortex core radius). During the time  $t = \frac{1}{v_{si}}$  spent by the loop in radial motion, the accumulated length parallel to the flow will be of the order of  $L_k = qv_{si}$ , where  $q = (1 - \frac{1}{2})$ . In the presence of counter flow  $v_{cf} = R$ , the helical distortions of the vortex, Kelvin waves, with wave vector  $k = L_k$  grow exponentially, if  $k < v_{cf} = 0$ . This condition is satisfied for  $q > 1$  independently of  $\frac{1}{2}$ . Thus at low damping a vortex becomes unstable with respect to the growth of Kelvin waves. These waves may reconnect with the boundary, increasing the number of vortices and providing new seeds for vortex multiplication. This scenario is similar to vortex multiplication which was seen in the simulations of Ref. [2] in a special vortex-like rotating flow field without boundaries. The required flow velocity is determined by the condition  $L_k = R$  which gives a low minimum value  $v_{cf} = R = 10^{-3}$  cm/s.

Two configurations have been identified in the experiment where curved vortices attached to the cylindrical sample boundary are expected to exist. One case is the equilibrium vortex state at  $\omega_i > 0$ . Here some outermost vortices may connect to the side wall since our cylindrical sample is only approximately aligned parallel to the rotation axis, with a precision of roughly one degree, see Fig. 1.

The other configuration includes remnant vortices at  $\omega_i = 0$ . When rotation is stopped, vortices are pushed owing to their mutual repulsion to the boundaries for annihilation. While most vortices decay rapidly, the annihilation time of the last few vortices becomes long below  $0.5 T_c$  owing to the small  $\frac{1}{2}$ . A straight vortex parallel to the cylinder axis at a distance  $b = R$  from the center survives for a time  $t = 2R^2 = (\frac{1}{2})[\ln \frac{1}{2}(1 - \frac{1}{2})]$ , where the prefactor equals 1 h at  $0.4 T_c$ . If the time spent at standstill before increasing rotation to  $\omega_f$  is significantly shorter, as in Fig. 2, then some vortices will stay in the

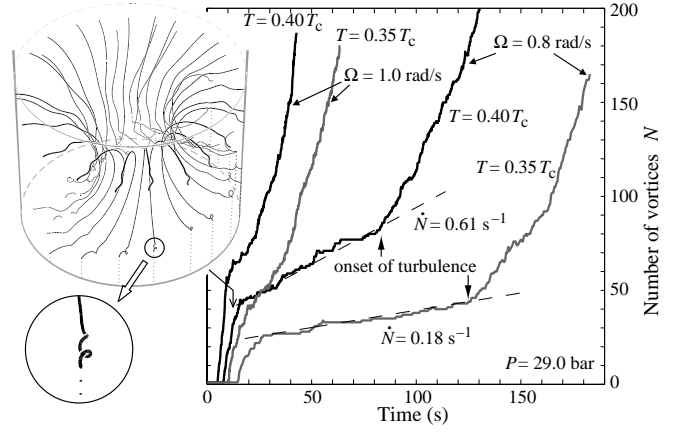


FIG. 3: Calculated vortex dynamics displays vortex formation which resembles the experimental observations in Fig. 1. The growth in the number of vortices  $N(t)$  in a cylinder with radius 3 mm and length 10 mm rotating with constant angular velocity is started from an artificial configuration: One vortex ring with radius 2 mm is placed in the azimuthal plane 2 mm above the bottom plate with its center displaced by 0.3 mm from the cylinder axis. The ring is unstable in the azimuthal counter flow and generates via the Kelvin wave instability tens of vortices in a rapid burst, which results in the configuration shown in the insert. After the burst the slow vortex formation at constant average rate  $\dot{N}$  starts. During this linear stage each new vortex is produced from the Kelvin-wave excitation on an isolated vortex line (like the one shown in the bottom insert) which is blown up to ring-like shape and then reconnects to the boundary. In the rapid turbulent growth, which occurs later, inter-vortex interactions and production of new vortices in the bulk become important.

sample. According to our numerical calculations they are attached to the sample boundary and are likely to have complex shapes. We argue that remnant vortices in our experiments have this dynamic character instead of being stationary pinned vortices: Above  $0.6 T_c$  no evidence exists for pinning, since vortices are formed at a well defined high critical velocity, which is explained by the instability of the bulk flow. It is not expected that pinning should have such a strong temperature dependence as observed in Fig. 2. For the same reason a vortex mill, with repetitive motion of a pinned vortex, can be excluded as a source of vortex formation in our measurements [3]. There is clear experimental evidence that the transition in Fig. 2 is shifted to lower temperatures if the waiting time at  $\omega_i = 0$  is increased, which is consistent with the dynamical nature of the remnant vortices.

Vortices, which are attached to the cylindrical sample boundary in the initial state at  $\omega_i$ , will spend a long time  $t = \frac{1}{\omega_f R}$  to expand axially along the sample column after rotation is increased to  $\omega_f$ . During this time they will move in the counter flow created by the rotation and may act as seeds for vortex formation in a manner described above.

These arguments provide a general picture of the vor-

tex multiplication which explains such experimentally observed features as the abrupt temperature dependence and the low threshold velocity. However, to understand more features, such as the constant growth rate  $N$  or the role of the interaction of a vortex moving close to the sample boundary with its image, we have examined vortex dynamics numerically.

**Simulations:** We used Eq. (1) with  $v_s$  obtained from the Biot-Savart law and an additional solution of the Laplace equation to satisfy the boundary conditions [11]. The sample is an ideal cylinder rotating around its axis. When the initial vortex configuration is carefully chosen, vortex formation similar to that observed in the experiment is obtained, Fig. 3. In particular, the slow stage with constant  $N$ , which precedes turbulence, is seen. The growth rate and duration of this stage are similar to the experimental values. The process which is responsible for vortex production in the pre-turbulent period involves expansion of Kelvin waves on the vortex ends which are attached to the sample boundary followed by reconnections with the boundary. The model for this process is studied in Fig. 4. Here the growth of the Kelvin waves strongly depends on the orientation of a vortex with respect to the flow. Appropriate orientations are more probable at low mutual friction damping which results in a temperature dependence similar to that observed in the experiment. The Kelvin waves are able to grow only on one of the two vortex legs formed in the reconnection. If the process occurs periodically then the increase of  $N$  is linear in time.

The agreement between the simulations and the experiment is not perfect: In simulations only a small set of artificial initial states leads to continuous growth of  $N$  as in Fig. 3, while configurations which are thought to be the seeds in the real experiment, like in Fig. 1, do not. The reason for this discrepancy is not understood. However, it is related to the following two properties of the simulated vortex dynamics: (i) In the pre-turbulent regime Kelvin waves are produced only when a vortex reconnects with the wall and sharp kinks are formed. These kinks are known to excite Kelvin waves [12]. (Although the reconnection procedure in simulations is always artificial we have checked that changing the reconnection distance from the wall by an order of magnitude does not change the results qualitatively.) (ii) The Kelvin wave excitations often reconnect to the wall too early, before expansion to a size of order  $R$ . In this case they do not have enough length along the flow to support the growth of new Kelvin waves from the reconnection kinks and vortex formation stops.

**Conclusions:** A vortex formation process, which precedes superfluid turbulence, is discovered in rotating  $^3\text{He-B}$  with applied flow. It operates at low vortex density and low flow velocity at temperatures  $T < 0.5 T_c$  if a vortex bending to the cylindrical sample boundary is present. We propose that such vortex multiplication proceeds via

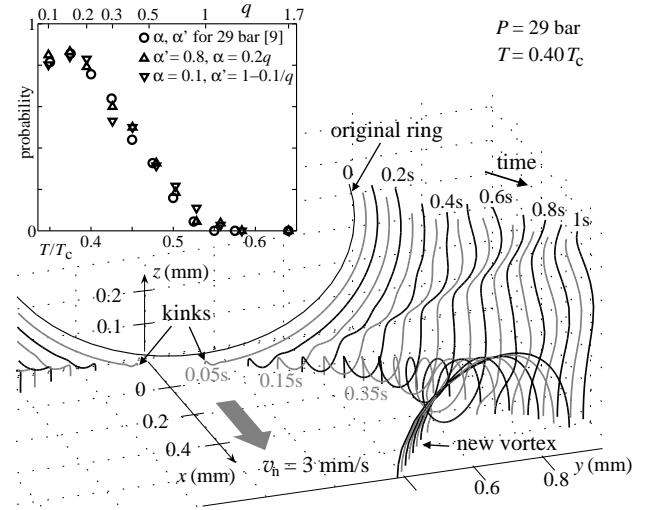


FIG. 4: Collision of a vortex ring expanding in applied flow with a wall. This is a model for the process which generates new vortices in the pre-turbulent regime of the simulations in Fig. 3. A vortex ring of radius 0.5 mm with its plane tilted by  $\approx 10^\circ$  from the  $x = 0$  plane is initially centered at  $z = 0.5$  mm above a wall at  $z = 0$ . In the frame of reference of this figure, uniform flow of the normal component at  $v_n = 3$  mm/s is applied in the  $x$  direction. The different contours show the evolution of the ring at 0.05 s intervals. The sharp kinks at the wall reconnections induce Kelvin waves on the ring. On the right hand side they grow in amplitude due to the interaction with the applied flow. The largest wave reconnects with the wall and a new vortex is separated from the original ring. The conditions for the growth of Kelvin waves, discussed in the text, are not always fulfilled in such collisions: The insert on the top shows the temperature dependence of the probability that a new vortex is created when the original ring is initially placed at  $z = 1$  mm with random orientation. This probability depends essentially on the ratio  $q = (1 - \alpha^2)/\alpha^2$ , shown on the top axis, rather than on  $\alpha$  or  $\alpha'$  separately. In the rotating flow in a cylinder the results remain qualitatively the same.

single-vortex processes: Kelvin waves grow on an existing vortex close to the sample boundary, reconnect with the surface, and produce a new vortex loop. This process is effective only at low mutual friction damping,  $q < 1$ .

This collaboration was carried out under the EU research programs ULTI-4 (RITA-CT-2003-505313) and ESF-CO SLAB.

- [1] K.W. Schwarz, Phys. Rev. B 31, 5782 (1985); Phys. Rev. Lett. 64, 1130 (1990).
- [2] D.C. Samuels, Phys. Rev. B 47, 1107 (1993).
- [3] V.M.H. Ruutu et al., J. Low Temp. Phys. 107, 93 (1997).
- [4] A.P. Finne et al., Nature 424, 1022 (2003); J. Low Temp. Phys. 138 (2005).
- [5] N.B. Kopnin, Phys. Rev. Lett. 92, 135301 (2004); V.S. L'vov et al., JETP Lett. 80, 479 (2004); L. Skrbek, JETP Lett. 80, 474 (2004); W.F. Vinen, Phys. Rev. B 71, 024513 (2005).

- [6] A.P. Finne et al., J. Low Temp. Phys. 135, 479 (2004);  
ibid. 136, 249 (2004).
- [7] J. Kopp et al., J. Low Temp. Phys. 120, 213 (2000).
- [8] R.J. Donnelly, Quantized Vortices in Helium II, p. 213  
(Cambridge University Press, Cambridge, UK, 1991).
- [9] T.D.C. Bevan et al., J. Low Temp. Phys. 109, 423 (1997).
- [10] R.M. Ostermeier, W.I. Glaberson, J. Low Temp. Phys.  
21, 191 (1975);
- [11] R. Hanninen et al., J. Low Temp. Phys. 138 (2005).
- [12] B.V. Svistunov, Phys. Rev. B 52, 3647 (1995); D. Kiv-  
otides et al., Phys. Rev. Lett. 86, 3080 (2001).